Materials Science Forum Vols. 389-393 (2002) pp. 1101-1104

Surface Morphology and Chemistry of 4H- and 6H-SiC After Cyclic Oxidation

Robert S. Okojie,[1] Dorothy Lukco,[2] Luann Keys,[1] Sergey Tumakha,[3] and Leonard J. Brillson [3]

[1] NASA Glenn Research Center, 21000 Brookpark Road, Cleveland OH, 44135, USA.

[2] AYT Research, Brookpark, OH 44142, USA

[3] Dept. of Electrical Engineering, The Ohio State University, Columbus, OH 43210, USA.

Keywords: Oxidation, surface morphology, surface chemistry, AFM, XPS, LEEN, CLS

Abstract. The analysis of the surface and sub-surface of n-type 6H- and 4H-SiC was performed after cyclic oxidation and oxide removal using X-ray photoelectron spectroscopy and multiple scans with atomic force microscope. The results reveal that the disappearance of C 1s binding energy spectral shoulders that arise from adventitious carbon and related compounds is tracked by the progression toward smoother surface morphology after more cycles of oxidation and oxide stripping. However, the 4H-SiC progression toward further smoothening was interrupted by sudden increase in roughness after the second cycle of oxidation and stripping, with a corresponding re-introduction of adventitious carbon. Low energy electron nanoluminescence spectra reveal prominent electronic states at 1.9 and 3.3 eV at the 6H/metal and 2.0 eV at the 4H/metal interface that are independent of the process steps.

Introduction

Wide bandgap electronics based on silicon carbide has evolved to the point that a few products are manufactured in commercial volume. Although desirable ohmic or Schottky characteristics are obtainable for SiC devices, the interface properties depend significantly on specific process conditions used to prepare them. Localized electronic states at these interfaces are sensitive to such processing and can have substantial effects on barrier properties. However, relatively little is known about SiC interfacial properties compared with more conventional semiconductors [1,2]. The altered atomic arrangements and chemical bonding can form electronic states near interfaces. These could be localized just a few monolayers from the semiconductor/metal junction, or buried nanometers below the interface. The inherent inhomogeneous electrical characteristics of the metal/SiC interface are still not well understood, despite various attempts at studying the surface characteristics [3]. Lebedev *et al.* [4] indicated that KOH etching of the surface lowered the barrier height more than plasma etching. Teraji *et al.* [5] attributed the formation of good ohmic contact to n-type 6H-SiC by making the surface 'atomically flat' via oxidation and HF etching and also via immersion in boiling water. However, the homogeneity of the metal/SiC electrical properties after these treatments was not determined.

Here we present results showing the effects of standard processing steps such as oxidation, HF strip, piranha-clean and metallization on the smoothening of the surface, formation of defect states and polytypic transformations near Pt/Ti/6H- and 4H-SiC interfaces. A correlation between surface morphology and surface chemical states in terms of how the coupling could affect the interfacial electrical characteristics is also presented. We depended on the anisotropic oxidation rates at the crystallographic planes [6] on off-axis 4H- and 6H-SiC to smoothen the surface by performing cyclic oxidation and oxide stripping. After each oxide stripping step, the interaction between surface morphology and surface chemistry was investigated with Atomic force microscopy (AFM) and X-ray photoelectron spectroscopy (XPS), respectively, while cathodoluminescence spectroscopy (CLS) using low electron-energy excited nanoscale luminescence (LEEN) was used to study the electronic states at the metal contacts to 6H- and 4H-SiC epilayers [7].

Experimental

Three samples were obtained each from wafers with 2 μm *n*-type epilayers of 6H-SiC (3.5° off-axis, doping level 2 x 10^{19} cm^{-3}) and 4H-SiC (8° off-axis, doping level 1.7 x 10^{19} cm^{-3}) grown on the respective 7 Ω cm and 4 Ω cm resistivity *p*-type substrates. After all the samples were cleaned in acetone and methanol (henceforth termed 'SC'), a sample from each polytype was put aside and the remaining four were dry oxidized at 1150°C for 4 hours. The oxide on the four samples was stripped in 49% HF, rinsed in deionized (DI) water and blow dried in nitrogen before dipping in 1:1 volume ratio of H_2SO_4 and H_2O_2 (p-clean) for 10 minutes (samples termed 'OSP-1'). A vigorous DI water rinse and nitrogen blow-drying followed, after which one sample of each polytype was put aside while the remaining two samples were returned for a second dry oxidation at 1150°C for 5 hours. The above process sequence of oxide stripping and p-clean was repeated on the final pair of samples (samples termed 'OSP-2'). Each pair of samples was immediately analyzed by XPS after the final nitrogen blow-drying step, followed by multiple area AFM scans. Another batch of three pairs of samples similarly processed at the same time as above was metallized by sputter deposition of Ti(10 nm)/Pt(20 nm), correspondingly termed SCM, OSPM-1, and OSPM-2, respectively. This batch of metallized samples was analyzed by CLS using LEEN.

Results and discussions

The morphological study was performed with multiple AFM scans across different 1 x 1 μm^2 areas on each 1 x 1 cm^2 sample in order to assure statistically valid results. The average root mean square (RMS) surface roughness after each cycle of OSP is shown in Figs. 1a and b for the 6H- and 4H-SiC samples, respectively. The 6H-SiC samples show the RMS surface roughness to average 0.58 nm after SC and gradually reduced to 0.4 nm after OSP-2. The roughness trend of 4H-SiC did not fully follow a similar trend. The average RMS roughness after SC was 0.4 nm and dropped to 0.26 nm after OSP-1. While multiple AFM scans were also performed on the 4H-SiC, only three gave acceptable values after the OSP-2 due to the phenomenon associated with stacking faults generation [8] that caused severe roughness as was

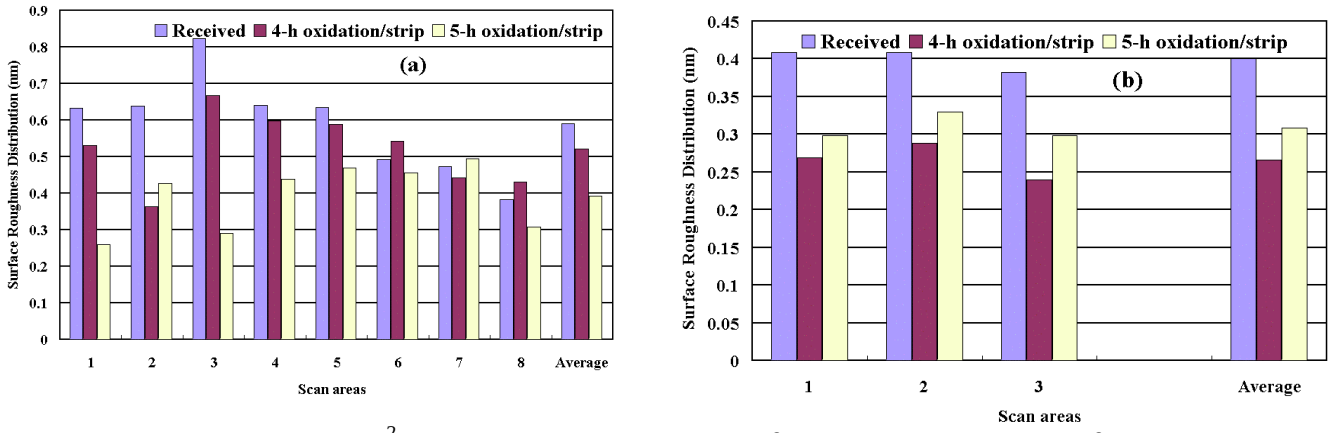

Fig. 1: *Multiple area 1 x 1 μm^2 AFM scan roughness data of a) 6H- and b) 4H-SiC after SC, OSP-1, and OSP-2. Note the contrast in surface smoothening between the two polytypes with the 4H-SiC exhibiting an irregular smoothening process with cyclic oxidation.*

manifested in the increase in average surface roughness to 0.31 nm after OSP-2 seen in Fig. 1b. As a result, without loss of data content, the multiple area scan data acquired after SC and OSP-1 was reduced to three (the average roughness of each of the first two multiple scans were the same as the average roughness when reduced to three) so as to harmonize them with the three AFM scans accepted after OSP-2.

The broad XPS survey spectra of the chemical species on the surface of both SC polytypes show up to 2.5 at. % chlorine present on the surface. The chlorine concentration dropped below detection limits (0.1%) after OSP-1. The C 1s spectra of both the SC 6H- and 4H-SiC samples are shown in Figs. 2a and b, respectively. In both SC samples, the C 1s core level peaks exhibit a dominant peak at 283.7 eV corresponding to bulk SiC, and a smaller shoulder at higher binding energy corresponding to near-surface adventitious carbon. After OSP-1, the XPS C 1s spectrum of the 6H-SiC polytype still shows adventitious

carbon as a higher binding energy shoulder while the C 1s spectrum of the 4H-SiC, on the other hand, shows a much cleaner carbide peak with minimal shoulder. However, after OSP-2, the 6H-SiC sample exhibited only the primary C 1s binding energy peak similar to the single C peak observed in 4H-SiC after OSP-1 as seen in Fig. 2b. The XPS spectra of C 1s on the 4H-SiC after OSP-2 reveals the introduction of extra binding energy peak in addition to the primary C 1s peak of 4H-SiC.

It is worth noting that after OSP-1, the 4H-SiC achieved a surface roughness (0.26 nm) close to the equivalent of a Si-C bilayer step height (0.25 nm) seen in Fig. 1b while it took the 6H-SiC sample until

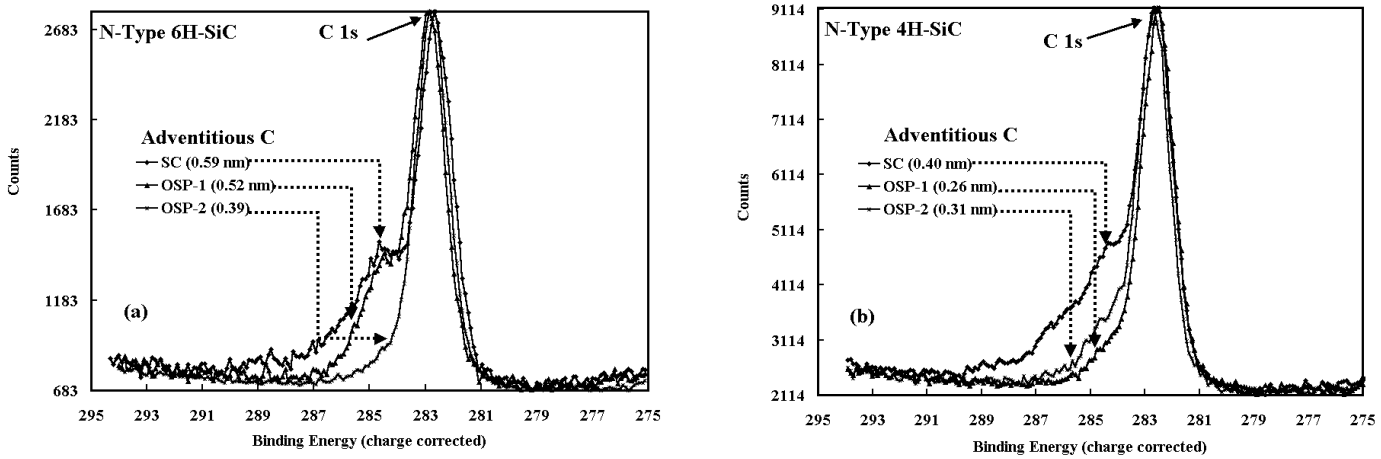

Fig. 2: *XPS of the C 1s binding energy spectra on the surface of a) 6H-SiC and b) 4H-SiC samples after SC, OSP-1, and OSP-2. Note the correlation between absence of adventitious carbon and the single bilayer equivalent surface roughness (0.25 nm) in Fig. 1. It takes two OSP's for 6H-, as against one OSP for 4H-SiC, to reach smoothest state.*

OSP-2 for its surface to acquire a surface roughness approaching a single Si-C bilayer as seen in Fig. 1a. The condition of a single bilayer equivalent surface roughness directly correlates with the greatly minimized presence of binding energy shoulder left of the C 1s corresponding to adventitious carbon.

The model suggested for the above phenomenon is explained briefly as follows: The step heights that are present as ridges on off-axis 6H- and 4H-SiC expose crystallographic planes other than the basal plane, thereby increasing the surface area. These exposed planes (e. g $\langle 11\bar{2}0 \rangle$) form an angle with the basal plane (terrace) and therefore provide localized high surface energy along the 'ridges' that promote reaction between adventitious carbon, oxygen, and the carbon atoms terminated on the $\langle 11\bar{2}0 \rangle$ plane. In addition, it is well known that reaction kinetics are more enhanced as the reaction surface area increases [9]. This model is validated on the 6H-SiC by the disappearance of the adventitious carbon after OSP-2 as the surface roughness reduced further (lower step height) and by its re-appearance on the 4H-SiC after OSP-2 as the surface roughness increased. Assuming that the C 1s peak is indicative of surface states, then the reduction in the higher binding energy shoulder with oxidation is consistent with removal of adventitious carbon.

LEEN measurements taken over a range of incident electron beam energies provide a means to identify the presence of localized states and their spatial distribution on a nanometer scale. With increasing excitation energy, E_B, the electron cascade and resultant generation of free electron-hole pairs occur at increasing depths, ranging from 25 nm at 1 keV to 150 nm at 4 keV for SiC's nucleon values and material densities. Electron-hole excitation rates peak at values U_0 that are one-third of these depths. Figures 3a and b illustrate the LEEN features at the metal interfaces with the 6H- and 4H-SiC polytypes after the various cyclic steps, respectively. The presence of the 1.9 eV LEEN feature at the 6H-SiC interface after OSP-1 coincides with the appearance of additional higher C binding energy peak associated with adventitious carbon in the 6H-SiC (Fig. 2a). It, however, does not explain the broad 2.0 eV emissions in the 4H-SiC after similar process step, which is free of adventitious C binding energy peak (Fig. 2b) correlating to the 0.26 nm surface of Fig. 1b. The 1.9 eV and the 2.0 eV features can be attributed to electronic states near midgap that are enhanced after OSP-1 cycle, and appear independent of surface morphology. This suggests

that the 1.9 and 2.0 eV features are due to other mechanisms. Fermi level "pinning" by discrete states located 1.9 eV below the conduction band edge would contribute to n-type Schottky barriers. Previous work [10] indicated Fermi level positions 1.8-2.0 eV above the valence bandedge for Ti on n-type 6H-SiC. The correspondence with the 1.9 eV emission provides modest evidence for the midgap states contributing to Fermi level pinning. Its absence after OSP-2 suggests that lattice damage and/or contamination removed by the second oxidation. The continuum of states within the band gap at the metal interfaces of both 6H-SiC and 4H-SiC is consistent with a disordered interface and a distribution of localized states [11].

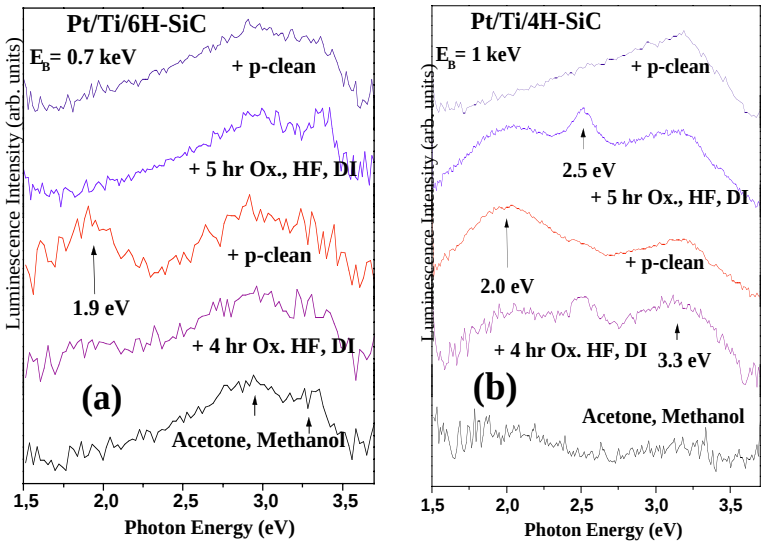

Fig. 3: *LEEN spectra directly under the metal interface with a) 6H-SiC show that 1.9 eV and 3.3 eV features are relatively independent of process; b) 4H-SiC show the 2.0 eV midgap state also believed to be independent of surface morphology.*

Conclusion

The inhomogeneous electrical characteristics of metal/SiC interfaces may not be attributed to a single mechanism. It will be necessary to de-couple the mutual interactions between mechanisms such as surface morphology and surface chemistry in order to determine which is the more dominant. We have shown that surface smoothening by oxidation, HF-strip, and p-clean creates a low surface energy that inhibits adventitious carbon compounds. Therefore, observed variations in surface roughness across the samples may contribute to inhomogeneous electrical characteristics from device to device. While the correlation between surface morphology and surface chemistry appears stronger in 6H-SiC, the 4H-SiC sample appears to be more chemically and electronically sensitive to surface perturbations. From this result, we also infer that mechanisms such as surface disordering and associated nonuniform distribution of surface states could also be contributing factors that are exclusive of surface roughness.

Acknowledgements

This work is supported by NASA under the Glennan Microsystems Initiative (GMI). LJB acknowledges additional support from the Office of Naval Research and the Air Force Office of Scientific Research. The NASA internal technical review by Drs. Phil Neudeck, Larry Matus, and Jih-Fen Lei is also acknowledged.

References

[1] M. J. Bozack, Phys. Stat. Sol.(b) **202**, pp. 549 (1997).
[2] H. Morkoc, S. Strite, G.B. Gao, M.E. Lin, B. Sverdlov, and M. Burns, *J. Appl. Phys.* **76**, pp. 1363 (1994).
[3] D. Defives, O. Noblanc, C. Dua, C. Brylinski, M. Barthula, V. Aubry-Fortuna, and F. Meyer, *IEEE Trans. Elect. Dev.* **46** (3), pp. 449 (1999).
[4] A. A. Lebedev, D. V. Davydov, V. V. Zelenin, and M. L. Korogodskiĭ, *Semiconductors*, **3** (8), pp. 875 (1999).
[5] T. Teraji, S. Hara, H. Okushi, and K. Kajimura, *Appl. Phys. Lett.* **71** (5), pp. 689 (1997).
[6] J. N. Shenoy, M. K. Das, J. A. Cooper, Jr., M. R. Melloch, and J. W. Palmour, J. Appl. Phys. **79** (6), pp. 3042 (1996).
[7] T. M. Levin, G. H. Jessen, F. A. Ponce, and L. J. Brillson, *J. Vac. Sci. Technol.* B **17** (6), 2545 (1999).
[8] R. S. Okojie, M. Xhang, P. Pirouz, S. T., and L. J. Brillson, In this proceeding.
[9] D. D. MacNeil, D. Larcher, and J. R. Dahn, *J. Electrochem. Soc.*, **146** (10), pp. 3596-3602 (1999).
[10] J.R.Waldrop and R.W.Grant, *Appl. Phys. Lett.* **62**, pp. 2685 (1993).
[11] H. Hasagawa and H. Ohno, *J. Vac. Sci. Technol.* **B4**, pp. 1130 (1986).